Origin of the 100,000-year timescale in Antarctic temperatures and atmospheric CO_2

J. R. Toggweiler[1]

[1] A new mechanism is proposed to explain the 100,000-year timescale for variations in Antarctic temperatures and atmospheric CO_2 over the last 650,000 years. It starts with fluctuations in the oceanic overturning around Antarctica that release CO_2 up to the atmosphere or trap it in the deep ocean. Every 50,000 years one of these fluctuations coincides with a changeover in the burial of $CaCO_3$ in the deep ocean. The changeover alters the atmospheric pCO_2 in a way that augments the tendency of the overturning. The augmented overturning then enhances the tendency of the $CaCO_3$ burial, which augments the overturning, etc. In this way, an individual random fluctuation becomes one of the big transitions seen in the Antarctic ice cores. Alternating transitions toward the warm and cold states every 50,000 years produce the 100,000-year timescale. The 50,000-year time interval is set by the turnover time for $CO_3^=$ ions in the ocean with respect to the CO_2-induced weathering of silicate rocks and the burial of $CaCO_3$ on the seafloor.

Citation: Toggweiler, J. R. (2008), Origin of the 100,000-year timescale in Antarctic temperatures and atmospheric CO_2, *Paleoceanography*, *23*, PA2211, doi:10.1029/2006PA001405.

1. Introduction

[2] The most intriguing result to come from the ice cores drilled in Antarctica is a pair of highly correlated cycles in atmospheric CO_2 and Antarctic temperatures seen in Figure 1 [after *Petit et al.*, 1999]. The air temperature in the top curve varies through four sawtooth-shaped cycles with a duration of about 100,000 years. Abrupt warmings of $8-10°C$ lead off each 100,000-year cycle. Atmospheric CO_2, on the bottom, rises and falls by 100-ppm in a similar way.

[3] Sawtooth-shaped cycles of this duration are also seen in Northern Hemisphere ice volume [*Shackleton*, 1967; *Imbrie et al.*, 1984]. In this case, the northern ice sheets seem to grow slowly and then melt back during events called terminations in which almost all the northern land ice abruptly melts away [*Broecker and van Donk*, 1970]. Northern terminations occur around the same time as the abrupt warmings in Antarctica.

[4] These cycles are too peculiar to have arisen independently. So, from which hemisphere does the 100,000-year cycle arise? The prevailing view is that the cycle of ice volume is regulated in some way by a 100,000-year cycle in the eccentricity of the Earth's orbit, which alters the insolation over the northern ice sheets [*Hays et al.*, 1976]. If so, the cycles in the north must be initiating the cycles in the south.

[5] In fact, the opposite seems to be true. Ice volume is recorded in the $\delta^{18}O$ of sand-sized carbonate shells in marine sediments. The $\delta^{18}O$ in this case is influenced by both the volume of northern ice and the temperature of the water in which the shells were formed. *Shackleton* [1987, 2000] has shown that much of the 100,000-year variability in "northern ice volume" is actually due to 100,000-year oceanic temperature variations that track the temperatures in Antarctica in Figure 1. When temperature and ice volume are resolved in the same records, as in Figures 3 and 4 of *Lea et al.* [2000], southern warming occurs well before northern melting. Southern temperatures also have more of the characteristic sawtooth shape. Thus, the peculiar 100,000-year cycle would appear to have its origin in the Southern Hemisphere.

[6] Much of the CO_2 added to the atmosphere in Figure 1 comes from CO_2 that is respired from sinking particles in the deep ocean [*Broecker*, 1982]. Respired CO_2 builds up in the deep ocean during cold glacial periods and is then vented up to the atmosphere around Antarctica when Antarctica warms [*Hodell et al.*, 2003]. *Shackleton* [2000] suggested that the eccentricity is somehow regulating the biogeochemistry of CO_2. The temperatures in Antarctica and across most of the ocean are then picking up the 100,000-year eccentricity period as a greenhouse response to CO_2.

[7] Shackleton does not say how or why the biogeochemistry of CO_2 should be responding to eccentricity variations. He also makes a wrong prediction. By saying that the warming in Antarctica is a greenhouse response to CO_2 he implies that CO_2 is increasing first in Antarctica. In fact, Antarctic temperatures have been shown to rise slightly ahead of CO_2 [*Fischer et al.*, 1999; *Caillon et al.*, 2003].

[8] This paper puts forward a different kind of Southern Hemisphere approach. It follows up on an idea in *Toggweiler et al.* [2006] that Antarctic air temperatures and atmospheric CO_2 vary together because they respond in a similar way to an internal mechanism that operates in the ocean and atmosphere around Antarctica. This paper shows that the internal mechanism has an intrinsic timescale of 100,000 years, which means that the 100,000-year cycles and the big

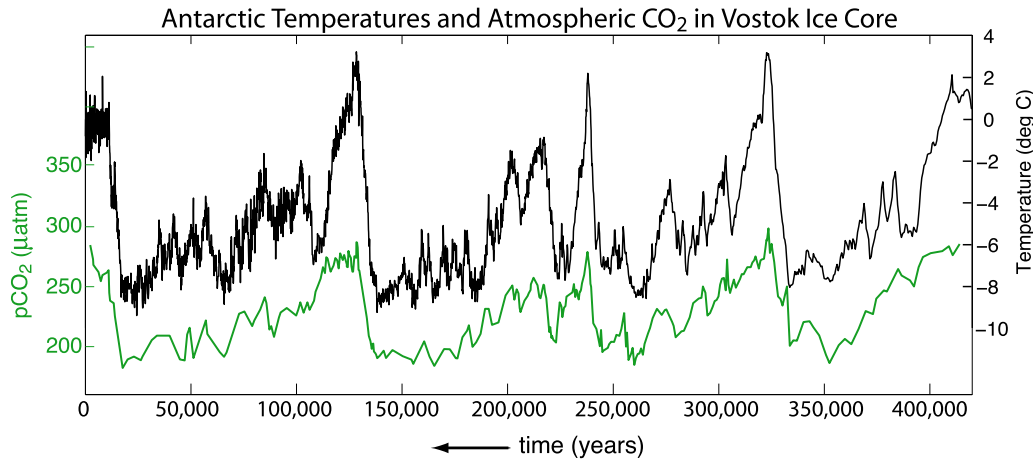[1]Geophysical Fluid Dynamics Laboratory, NOAA, Princeton, New Jersey, USA.

Figure 1. Antarctic air temperature (top curve) and atmospheric pCO_2 (bottom curve) over the last 430,000 years [after *Petit et al.*, 1999].

transitions in Figure 1 are not derived from the orbital forcing or the northern ice sheets.

2. Internal Mechanism

[9] The ocean's polar regions tend to be low in salinity because the precipitation and runoff in these areas exceeds the evaporation. Low polar salinities make polar surface waters less dense and less likely to sink. With less polar sinking, there is less overturning and less ventilation of the deep ocean.

[10] *de Boer et al.* [2007] showed recently that the salinity effect on the overturning around Antarctica is relatively unimportant when the ocean is warm but becomes more and more important as the ocean's polar temperatures approach the freezing point. The overturning tends to be strong when the mean polar temperature is more than a few degrees above 0°C and is very weak when the polar temperature is below 0°C. The overturning strength is particularly sensitive to salinity changes (i.e., unstable) when polar temperatures fall in an intermediate range between, say, 1 and 3°C.

[11] In this regard, the Earth has been gradually cooling over the last 50 Ma [*Zachos et al.*, 2001] in response to lower and lower levels of atmospheric CO_2 [*Berner*, 1991; *Lowenstein and Demicco*, 2006]. Changes in the atmospheric pCO_2 like these are determined by the "slow processes" of the CO_2 system − volcanism, weathering, and the burial of $CaCO_3$ on the seafloor. The specific hypothesis put forward here is that the overturning and ventilation around Antarctica became unstable about a million years ago when the mean pCO_2 dictated by the slow processes fell to around 225–230 ppm and brought the Earth's polar ocean temperatures into the unstable intermediate range.

[12] CO_2 is shifted from the deep ocean up to the atmosphere when the overturning around Antarctica strengthens and is shifted from the atmosphere down to the deep ocean when the overturning weakens [*Toggweiler*, 1999]. When combined with the warming (cooling) effect of having more (less) CO_2 in the atmosphere, this relationship should produce a positive feedback that reinforces the warm "on" and cold "off" states on either side of the intermediate range

and it should sharpen the unstable intermediate state into something that is more threshold-like [*Toggweiler et al.*, 2006].

[13] This means that the atmospheric pCO_2 should jump up and down about the mean pCO_2 favored by the slow processes. When the slow processes manage to bring the pCO_2 and the polar temperatures back to 225–230 ppm, which they will inevitably manage to do, the overturning and pCO_2 are compelled to flip to the other state. Thus, changes in the overturning and atmospheric CO_2 are inherently cyclic, and the cyclic behavior is likely to have an internal timescale that is set in some way by the slow processes.

[14] The basic idea, in full, is that (1) the modern climate has a baseline pCO_2 somewhere around 225–230 ppm that is set by volcanism and weathering, (2) the overturning/ventilation around Antarctica tends to switch around the baseline, (3) 50,000 years is required to set up the system for the next flip of the switch. Two flips of the switch, one in the warm direction, one in the cold, make up the 100,000-year cycle.

[15] Section 3 describes the slow processes. A box model that includes the slow processes is described in section 4 and is used in section 5 to produce synthetic 100,000-year cycles. The model does not attempt to explain the sawtooth shape. The discussion in section 6 revisits observations and ideas about the 100,000-year cycle in light of the model results.

3. Slow Processes of the CO_2 System

[16] The most important source of CO_2 to the atmosphere over long periods of time is the output of CO_2 from volcanoes and tectonic activity. The most important sink is the weathering of silicate rocks. The CO_2 removed from the atmosphere by weathering enters the ocean as HCO_3^- in river water along with the alkaline residues of the weathering process. The turnover time for the CO_2 in the ocean and atmosphere with respect to volcanism and weathering is about a half million years [*Walker et al.*, 1981].

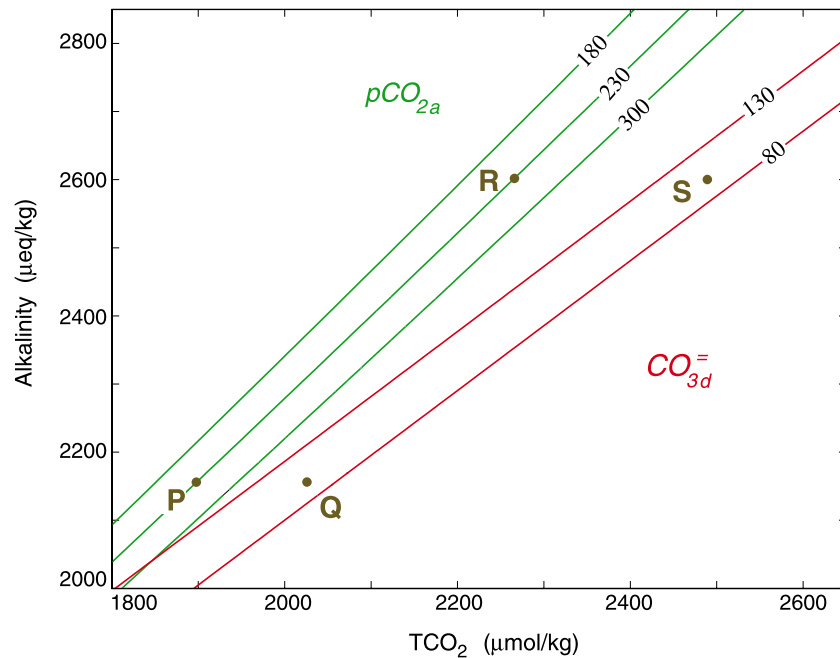[17] *Walker et al.* [1981] argued that volcanism and weathering are constantly damping the atmospheric pCO_2

Figure 2. Schematic diagram showing how the pCO_2 and $CO_3^=$ contents of the surface and deep ocean vary with respect to the alkalinity and TCO_2. The alkalinity and TCO_2 of the surface ocean are constrained in the model to lie along the green 230-ppm pCO_2 contour while the alkalinity and TCO_2 of the deep ocean are constrained to lie along the 90 μmol kg^{-1} $CO_3^=$ contour (between the red 80 and 130 μmol kg^{-1} contours). Points P and Q give the positions of the surface and deep ocean today in relation to the surface and deep water in the glacial ocean, points R and S. The pCO_2 and $CO_3^=$ isolines in Figure 2 were determined at the same temperature to limit the lateral spread between the sets of isolines.

toward a steady state value where the volcanic CO_2 source and the weathering sink come into balance. The key to this kind of feedback is that weathering rates increase with the pCO_2. *Berner* [1998] and *Moulton and Berner* [1998] argued that the Walker et al. feedback is mediated through the activity of land plants. Higher CO_2 stimulates plant growth by making more CO_2 available for photosynthesis and by making the Earth warmer and wetter. More plant growth leads to more acid respiration in the soil and more weathering.

[18] The damping time for the *Walker et al.* [1981] feedback should be about 350,000 years. Our longest record of atmospheric CO_2, at 650,000 years [*Siegenthaler et al.*, 2005], is nearly twice the damping time. It is noteworthy in this respect that the CO_2 maxima and minima over the last 650,000 years are quite similar from one cycle to the next and that the mean pCO_2 is remarkably constant near 225–230 ppm. The record is therefore consistent with the Walker et al. idea: something seems to be constraining the pCO_2 over a timescale that is commensurate with the length of the record (650,000 years) but longer than the CO_2 anomalies within each 100,000-year cycle.

[19] Weathering is also affected by tectonics, specifically the rate at which unweathered silicate rocks are lifted up and exposed to mechanical erosion by running water, freezing, and thawing. *Raymo and Ruddiman* [1992] call upon this argument to explain the CO_2 reduction and cooling over the last 10–20 Ma. Tectonic factors are assumed here to provide a base level of weathering that has not varied over

the last million years. The base rate is then supplemented by a factor whose rate increases with the atmospheric pCO_2.

[20] The CO_2 put into the atmosphere by volcanoes is removed by the burial of $CaCO_3$ in the ocean's sediments. The oceanic factor that governs the preservation and burial of $CaCO_3$ is the $CO_3^=$ concentration of the deep water that is in contact with the sediments. The importance of $CO_3^=$ ion stems from its role in the chemical reaction, $Ca^{++} + CO_3^= \leftrightarrow CaCO_3(s)$.

[21] For a given volcanic output of CO_2 there is a particular $CO_3^=$ concentration, or set point, that allows the ocean to preserve or bury the right amount of $CaCO_3$. For the most part, the ocean holds its deep $CO_3^=$ near the set point through variations in its lysocline, which adjusts in a way that damps the $CO_3^=$ back to the set point [*Broecker and Peng*, 1987]. More $CaCO_3$ is buried when the $CO_3^=$ is above the set point; more is dissolved when the $CO_3^=$ is below. The nominal timescale for lysocline adjustments is about 5,000 years.

[22] For the purposes of the model below, the slow processes have been reduced to a pair of negative feedbacks that damp the atmospheric pCO_2 and the deep $CO_3^=$. The weathering feedback constrains the atmospheric pCO_2, and the pCO_2, in turn, constrains the CO_2 content of the ocean's surface waters. The $CO_3^=$ feedback constrains the deep $CO_3^=$, and the deep $CO_3^=$, in turn, constrains the CO_2 content of the ocean's deep water.

[23] Figure 2 is a property/property plot for the alkalinity and total CO_2 of seawater. Overlaid on the plot are a set of

isolines that connect alkalinity and TCO_2 compositions with the same pCO_2s and the same $CO_3^=$ concentrations. Thermodynamic relationships make the two sets of isolines diverge from each other up the plot.

[24] Damping the atmospheric pCO_2 and deep $CO_3^=$ is equivalent to making the alkalinity and TCO_2 compositions of the surface ocean and deep ocean, respectively, lie along a pair of these isolines. As mentioned above, changes in the overturning/ventilation around Antarctica shift respired CO_2 between the deep ocean and atmosphere; CO_2 shifts of this sort, by definition, knock the surface and deep compositions off the isolines in opposite directions.

[25] The 230-ppm and 90 μmol kg^{-1} isolines in Figure 2 are the particular isolines that are damped to in the model. Points P and Q on the plot have been drawn to represent the current ocean's surface and deep compositions at steady state. The system is currently in its warm state with an active overturning circulation around Antarctica. As such, the ocean has relatively little respired CO_2 at depth. This means that the TCO_2 difference between the upper ocean and deep ocean is currently rather small, $\sim$120 μmol kg^{-1} [*Toggweiler et al.*, 2003]. As a result, points P and Q sit relatively low on the plot where the horizontal spread between the steady state pCO_2 and $CO_3^=$ isolines is relatively small.

[26] The overturning during the last glacial period was very weak or completely shut down. As a result, the surface to deep TCO_2 difference was about 220 μmol kg^{-1}, 100 μmol kg^{-1} larger than at present [*Broecker*, 1982; *Toggweiler et al.*, 2003]. With the surface and deep compositions constrained as shown, the steady state composition for the glacial state lies up the plot where the spread between the isolines is larger, i.e., somewhere near the points R and S.

[27] The points P and Q and R and S are the steady state compositions that the ocean would have if the overturning stayed on or off for a very long time. As is evident from Figure 2, any attempt to reach these states involves a change in the total amounts of alkalinity and total CO_2 in the ocean. The nominal timescale for a full change of this sort would be about 500,000 years, the turnover time for CO_2 with respect to the slow processes.

[28] As shown in the model below, the more relevant timescale is the turnover time for the ocean's $CO_3^=$ with respect to the slow processes. As the $CO_3^=$ in seawater makes up only 10% of the ocean's total CO_2, the adjustment time is 10% of the total turnover time, or 50,000 years.

4. Model

4.1. Overview

[29] The model in this paper is based on the seven-box model of *Toggweiler* [1999] (Figure 3). The basic model is modified here to include a crude ventilation switch and simple treatments of weathering and $CaCO_3$ burial. The model is limited to the CO_2 system and the pCO_2 changes generated in the model are symmetric about the baseline.

[30] The model divides the ocean's interior between a mid depth box and a deep box. The mid depth box, a, is the domain of the deep water formed in the North Atlantic. The deep box, d, is the domain of deep water formed around
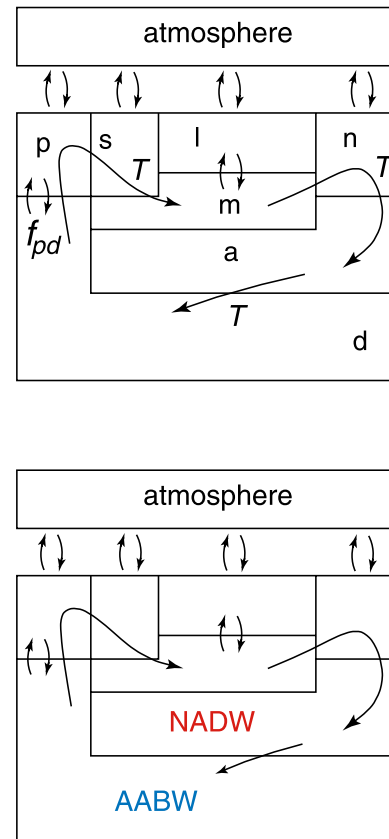

Figure 3. Box configuration for the seven-box model of *Toggweiler* [1999]. (top) Box labels and the main circulation/ exchange terms. (bottom) Box associations with the main oceanic water masses.

Antarctica. The formation and circulation of North Atlantic deep water is depicted by the circulation T. The formation and circulation of the deep water around Antarctica is represented by the ventilation parameter, f_{pd}. f_{pd} is the only parameter in the model that changes with time. T is held constant at 20 Sv (1 Sv = 1 × 10^6 m^3 s^{-1}). All the $CaCO_3$ sediments in the ocean are assumed to reside in the model's deep box.

[31] The base model here is identical to the 1999 original except that the thicknesses of the a and d boxes are reversed. The mid depth a box here is 1000 m thick and the deep box is 2000 m thick. This gives the upper ocean boxes, l, m, and a, a combined thickness of 2000 m, the same thickness as the d box. Model parameters are given in Tables 1–4 of *Toggweiler* [1999].

4.2. Treatment of Weathering

[32] *Walker and Kasting* [1992] described the weathering of silicate and carbonate rocks in a box model of similar complexity. Their scheme has been adopted here. It starts with a volcanic source, VDG, a constant addition of CO_2 to the atmospheric box per unit time. Alkalinity and CO_2 are then added to the low-latitude surface box, l, to represent the input of weathering products to the ocean in river water.

[33] The CO_2 input due to carbonate weathering is given by RVCARB in (1).

$$RVCARB = WCARB \times pCO_{2a} \times VL \qquad (1)$$

[34] WCARB is the weathering slope with respect to atmospheric CO_2 and VL is the volume of the low-latitude surface box, 2.62×10^{16} m^3. With WCARB = 2.0 mol m^{-3} atm^{-1} a^{-1}, the weathering of carbonates adds 14.7×10^{12} mol of CO_2 to the ocean per year at the preindustrial pCO_2 of 280×10^{-6} atm. The weathering of carbonates is a minor factor because it does not remove the CO_2 added to the atmosphere from the volcanic source.

[35] The CO_2 input by silicate weathering is given by RVSIL in (2), where the expression used by *Walker and Kasting* [1992] has been modified slightly.

$$RVSIL = (BSIL + WSIL \times pCO_{2a}) \times VL \qquad (2)$$

[36] The overall weathering rate in (2) is divided between a part that is constant and one that varies with the atmospheric pCO_2. The parameter BSIL in (2) is the constant part. It has a value of 0.75×10^{-4} mol m^{-3} a^{-1}. The parameter WSIL gives the change in weathering rate per unit pCO_2. It has a value of 0.5 mol m^{-3} atm^{-1} a^{-1}.

[37] Equations for the time evolution of alkalinity and TCO_2 in the low-latitude surface box are given in (3) and (4),

$$dAlk_l/dt = 1/VL \times (f_{lm} \times (Alk_m - Alk_l)$$
$$- r_{Alk:P} \times P_l + 2 \times (RVCARB + RVSIL)) \qquad (3)$$

$$dTCO_{2l}/dt = 1/VL \times (f_{lm} \times (TCO_{2m} - TCO_{2l})$$
$$- r_{C:P} \times P_l + RVCARB + RVSIL$$
$$+ \text{gas exchange}) \qquad (4)$$

where f_{lm} represents the exchange of water between the thermocline and low-latitude surface boxes and the P_l terms represent the uptake of alkalinity and CO_2 into sinking particles.

[38] With the parameters used in (2), RVSIL in (4) nominally adds 5.63×10^{12} mol of CO_2 to the ocean per year at a pCO_2 of 280×10^{-6} atm, about 1/3 of the CO_2 input from RVCARB. However, an amount of CO_2 equal to RVSIL is subtracted from the atmospheric box every time step to reflect the uptake of CO_2 during the weathering of silicate rocks. Thus, the removal of RVSIL from the atmosphere negates the addition of RVSIL to the ocean in (4). The net effect of silicate weathering is to increase the alkalinity of the ocean by $2 \times$ RVSIL in (3). Volcanic CO_2 is drawn into the more alkaline ocean by gas exchange.

[39] The input of volcanic CO_2 to the atmosphere, VDG, is determined by plugging 230×10^{-6} atm for pCO_{2a} into (2). This yields 4.98×10^{12} mol a^{-1}, the CO_2 input needed to balance the uptake of CO_2 by the weathering of silicate

rocks at 230 ppm. The input of volcanic CO_2 in the model is close to the estimated CO_2 release from volcanism and tectonics of 6×10^{12} mol a^{-1} given by *Marty and Tolstikhin* [1998].

[40] VDG and RVSIL damp the atmospheric pCO_2 back to 230 ppm. When the pCO_2 is below 230 ppm, the CO_2 added to the atmosphere exceeds the loss due to weathering. The larger volcanic source then gradually raises the pCO_2 back up to 230 ppm. When the pCO_2 is above 230 ppm the larger weathering sink gradually lowers the pCO_2 back to 230 ppm.

4.3. Burial and Dissolution of $CaCO_3$

[41] The deposition of $CaCO_3$ on the seafloor is also treated as a linear damping process. In this case, the $CO_3^=$ content of the deep box back is damped back to a specified target. The damping operator, CDAMP, is given by (5) where CDTARG is the target $CO_3^=$ concentration, 85 μmol kg^{-1}.

$$CDAMP = WDAMP \times TCO_{2d}/CDTARG$$
$$\times (CO_{3\,d}^= - CDTARG) \times VD \qquad (5)$$

[42] CDAMP represents the addition or removal of $CaCO_3$ from the deep box by dissolution (when $CO_{3\,d}^= <$ CDTARG) and by burial in the sediments (when $CO_{3\,d}^= >$ CDTARG). WDAMP is the damping rate, 2×10^{-4} per year [after *Broecker and Peng*, 1987]. The factor TCO_{2d}/CDTARG in (5), scales WDAMP so that the $CO_3^=$ is actually restored with the specified timescale.

[43] Equations for the time evolution of alkalinity and DIC in the deep box are given in (6) and (7). The terms with P_l, P_s, P_n, and P_p represent the additions of alkalinity and TCO_2 from sinking particles. The factor γ is used to partition the sinking fluxes between the thermocline box and the deep boxes below.

$$dAlk_d/dt = 1/VD \times (T \times (Alk_a - Alk_d) + f_{pd}$$
$$\times (Alk_p - Alk_d) + r_{Alk:P} \times ((1 - \gamma) \times 0.5$$
$$\times (P_l + P_s) + (1 - \gamma) \times P_n + P_p) - 2$$
$$\times CDAMP) \qquad (6)$$

$$dTCO_{2d}/dt = 1/VD \times (T \times (TCO_{2a} - TCO_{2d}) + f_{pd}$$
$$\times (TCO_{2p} - TCO_{2d}) + r_{C:P} \times ((1 - \gamma)$$
$$\times 0.5 \times (P_l + P_s) + (1 - \gamma) \times P_n + P_p)$$
$$- CDAMP) \qquad (7)$$

[44] The damping operator in (4) is a surrogate for the ocean's lysocline adjustment. When a disturbance knocks the deep $CO_3^=$ away from CDTARG, the damping operator brings it back by burying or dissolving $CaCO_3$. The damping operator also removes $CaCO_3$ from the ocean to balance the inputs of alkalinity and CO_2 from volcanoes and weathering. This means that the deep ocean must stay a

Table 1. Southern Ventilation Strength as a Function of Atmospheric pCO_2

pCO_2 Range, ppm	Implied Polar Temperature	Ventilation/ Mixing Strength, Sv
>240	warm	high (60)
220–240	intermediate	medium (27)
<220	cold	low (10)

bit more alkaline than CDTARG in order to have a net burial of $CaCO_3$ that balances the volcanic output.

4.4. Switching Behavior in the Model

[45] The switching behavior in the model is introduced by assigning certain values to f_{pd}, the southern ventilation parameter, when the atmospheric pCO_2 falls within three different ranges, as shown in Table 1. f_{pd} is given a high value of 60 Sv when the pCO_2 is high and the climate is warm and it is given a low value of 10 Sv when the pCO_2 is low and the climate is cold. Volcanism and weathering draw the pCO_2 back into an intermediate range (220–240 ppm) where f_{pd} has an intermediate value.

[46] The switching behavior comes about because the pCO_2 and the ventilation do not stay in the intermediate state for very long. Imagine, for example, that the system is initially in the high mode (top row of Table 1) and that the weathering causes the pCO_2 to fall into the intermediate band. The ventilation then decreases from its high value to its medium value, which causes respired CO_2 to build up in the deep box and makes the pCO_2 fall even more. The ventilation then decreases again and the system is soon down into the cold low mode (bottom row of Table 1).

4.5. Noise in the Model

[47] The overturning in nature is presumably capable of changing between its "on" and "off" states over a certain range of pCO_2s and temperatures. The switching described above takes place, however, at two arbitrary transition points. The rigidity of this behavior can be easily circumvented by some noise in the system.

[48] Every 1000 years the model asks for a random real number, RN, between 0 and 1 and then multiplies the current value of f_{pd} in the table above by the factor $\exp^{(RN-0.5) \times SM}$ to produce perturbed values of f_{pd} as shown in (8). The factor

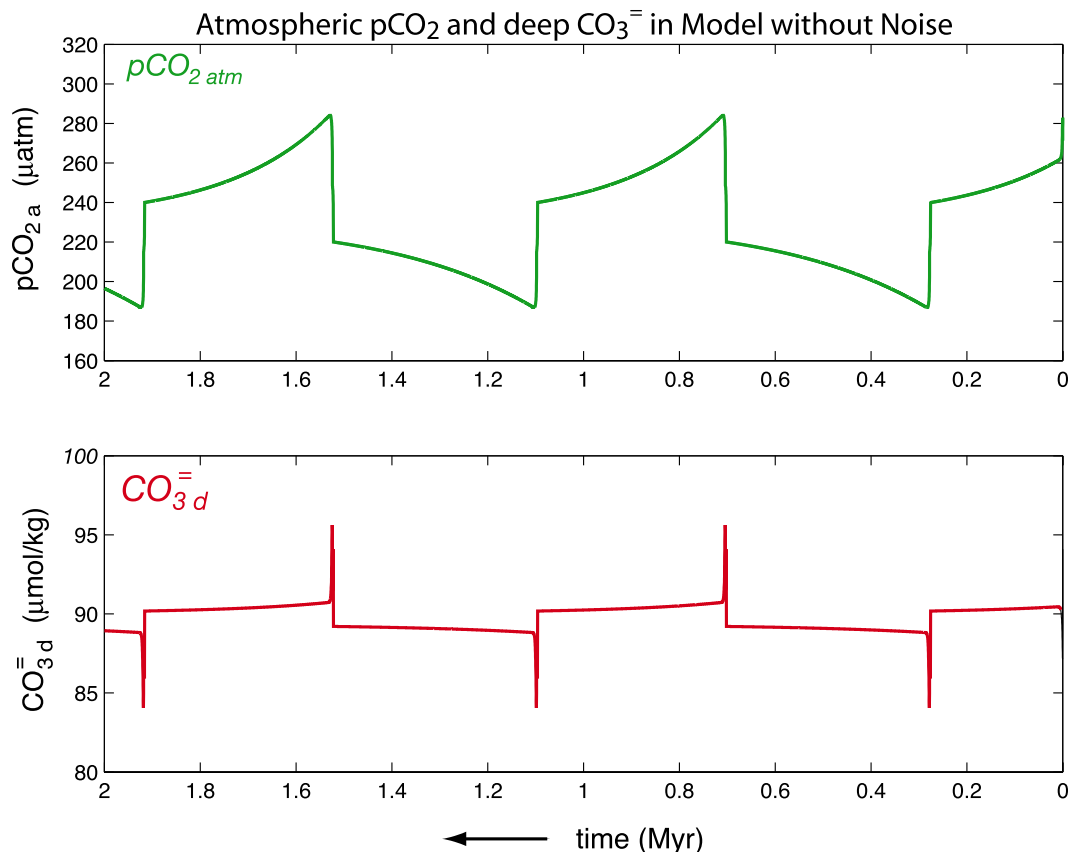**Figure 4.** (top) Synthetic cycles for the atmospheric pCO_2 and (bottom) deep $CO_3^=$ in a version of the model with the ventilation switch but no noise. A full cycle lasts 800,000 years and includes two abrupt transitions, one in the (warm) high-CO_2 direction and one in the (cold) low-CO_2 direction. Each transition is followed by a 400,000-year interval in which weathering and volcanism draw the pCO_2 back toward 230 ppm. The long-term mean $CO_3^=$ in the bottom plot is 89.7 μmol kg^{-1}, a value that exceeds the target $CO_3^=$ concentration in equation (5) by 4.7 μmol kg^{-1}. The continuous damping of this small excess provides the loss of CO_2 (via the burial of $CaCO_3$) that balances VDG, the volcanic CO_2 source.
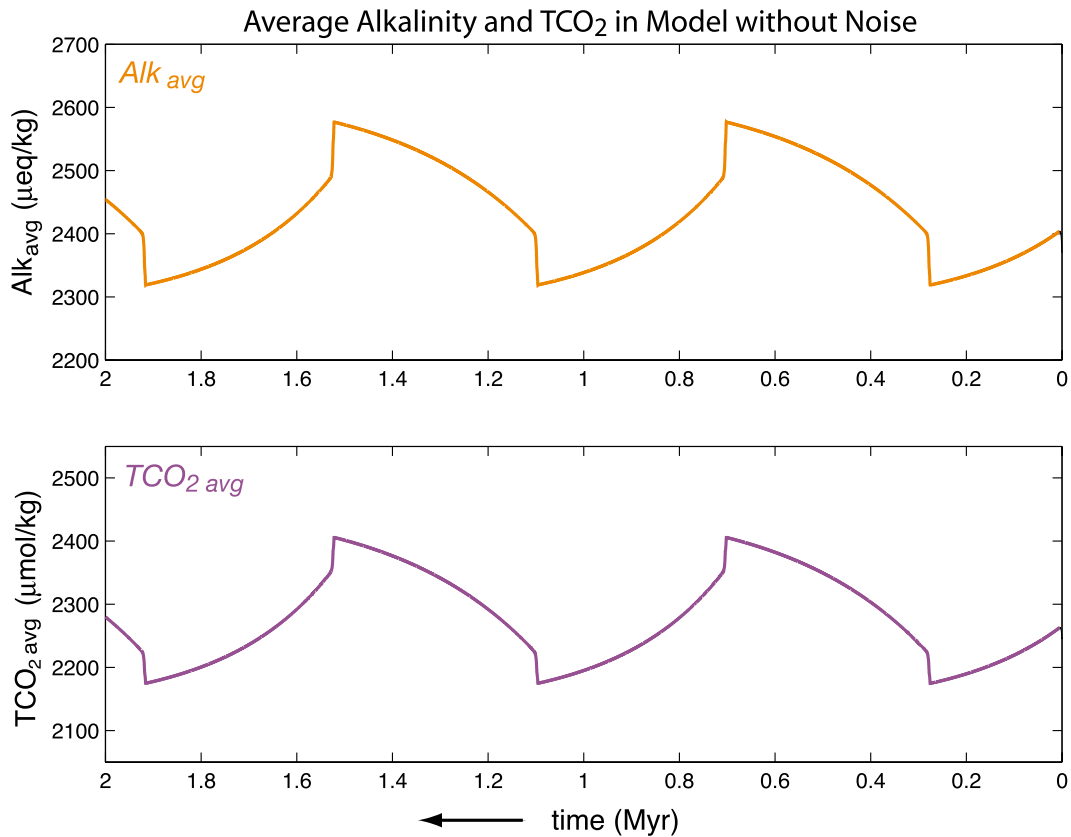
Figure 5. Average (top) alkalinity and (bottom) TCO_2 from all seven ocean boxes in a version of the model with the ventilation switch but no noise. The alkalinity and TCO_2 rise when the pCO_2 in Figure 4 decreases, and they fall when the pCO_2 increases. The alkalinity and TCO_2 keep rising and falling toward their warm and cold steady states as weathering and volcanism damp the pCO_2 back to its long-term mean.

SM scales the random multiplier. The base value in this example is 60 Sv.

$$f_{pd}(t) = 60 \times 3.1558 \times 10^{13} \text{ m}^3 \text{ a}^{-1} \times \exp^{(RN-0.5) \times SM} \quad (8)$$

[49] The average value of the random factor, $(RN - 0.5) \times SM$, is zero. The average value of the multiplier, $\exp^{(RN-0.5) \times SM}$, is 1.0. The perturbed values are therefore both larger and smaller than the base value.

5. Results

5.1. Slow Processes and the Ventilation Switch

[50] Figures 4 and 5 show the slow processes at work with the ventilation switch operating by itself. The noise is not active as the scaling factor SM in (8) has been set to 0. The switching behavior in this version of the model is dictated by the way that volcanism and weathering draw the atmospheric pCO_2 back to the transition points at 220 and 240 ppm.

[51] The model in this case produces a series of very long CO_2 cycles with a period of 800,000 years, as seen in Figure 4 (top). Volcanism and weathering take up most of the 800,000 years as they draw the pCO_2 back toward the steady state pCO_2 of 230 ppm. When the pCO_2 hits one of the transition points, the switch is activated and the pCO_2

quickly crosses over the unstable intermediate zone to the next "warm" or "cold" extreme. The pCO_2 is slowly drawn back again and the switch goes off in the other direction. Each drawing back phase takes 400,000 years.

[52] The ventilation switch itself accounts for only half of the pCO_2 jumps at the transition points. The other half is due to changes in $CaCO_3$ burial that take place in response to $CO_3^=$ changes in the deep box. Figure 4 (bottom) shows the $CO_3^=$ concentration in the deep box. Transitions into the warm high-CO_2 state begin with the venting of respired CO_2 up to the atmosphere. The loss of CO_2 raises the $CO_3^=$ concentration in the deep box, which leads to an increase in the burial of $CaCO_3$ via the damping operation in (5). The enhanced $CaCO_3$ burial removes alkalinity from the ocean, which effectively doubles the pCO_2 response to the initial venting of respired CO_2.

[53] Ocean chemists will recognize the effect of the $CO_3^=$ damping in Figure 4 as the $CaCO_3$ compensation mechanism of *Broecker and Peng* [1987]. The compensation step here comes to an end, however, before the deep $CO_3^=$ can be drawn all the way back to its long-term mean. This is because the two damping mechanisms come into conflict. By the time that the pCO_2 hits its warm peak (at 284 ppm) the deep $CO_3^=$ has fallen back to the point that the alkalinity removal due to $CaCO_3$ burial is offset by the alkalinity input to the ocean from weathering. The result is

a standoff in which further removal of $CaCO_3$ is unable to draw the deep $CO_3^=$ back to the long-term mean.

[54] Figure 5 shows the average alkalinity and TCO_2 of the ocean over the same time interval as Figure 4. The average alkalinity and average TCO_2 jump up or down initially in a 2:1 ratio in response to the initial damping of the deep $CO_3^=$. The alkalinity and TCO_2 then increase or decrease slowly together via changes that are nearly the same, i.e., in a 1:1 ratio. As a result, the amplitudes of the alkalinity and TCO_2 cycles in Figure 5 are similar, 260 μeq kg^{-1} for alkalinity and 230 μmol kg^{-1} for TCO_2. The alkalinity and TCO_2 are drawn toward the warm and cold steady states in Figure 2 during the standoff phase. The relative amplitudes in Figure 5 reflect the spread between P and Q and R and S in Figure 2.

5.2. Role of Fluctuations

[55] The ventilation switch in the previous section operated alone without the noise and fluctuations. The result is a series of very long cycles whose timescale is governed by volcanism and weathering.

[56] Figures 6a–6d show how a new timescale develops when the rigid behavior around the transition points is circumvented by noise. Figures 6a–6d show the model operating, first, with only the weathering feedback and the noise; second, with the ventilation switch active along with the noise; third, with the $CO_3^=$ feedback active; and finally, with the amplitude of the noise increased by 50%. Each result in Figure 6 shows the final 1.1 Ma of a 2 Ma model run.

[57] In Figure 6a, the volcanic CO_2 source operates along with the weathering feedback and the noise. The base value of f_{pd} is fixed and the scaling factor SM in equation (8) is given a value of 1.5. With this value of SM, the multiplier in (8) produces a series of small random pCO_2 variations about the steady state value (230 ppm) that just manage to touch the transition points at 220 and 240 ppm. Nothing happens here because the switch is not active, i.e., the base value of f_{pd} does not change when the pCO_2 hits the transition points.

[58] "Fluctuations" in the overturning occur when the switch is activated. The fluctuations appear in Figure 6b, where the base value of f_{pd} is allowed to change when the pCO_2 hits the transition points. The pCO_2 variations in this case are roughly twice as large as those in the first panel but are still rather small in relation to the observed cycles. Positive and negative fluctuations typically last for about 5,000 to 10,000 years as it takes several thousand years for respired CO_2 to build up or vent from the deep box.

[59] In Figures 6a and 6b the burial of $CaCO_3$ is set at a constant rate that balances the volcanic output. Thus, the burial of $CaCO_3$ does not change with the changes in ventilation. In Figure 6c the burial rate responds to the $CO_3^=$ concentration in the deep box via the damping operator in equation (5). The modeled pCO_2 variations become much larger in this case and reach the maximum and minimum values seen in Figure 4.

[60] The most noteworthy feature of the third panel is the way that $CaCO_3$ burial lengthens the cycles. Individual high-CO_2 and low-CO_2 intervals are up to 100,000 years long. Complete cycles last up to 200,000 years. In one sense, the situation in this time series has reverted back to the situation in Figures 4 and 5: the CO_2 cycles have become so large in relation to the fluctuations that the model is left waiting for volcanism and weathering to draw the pCO_2 back to the transition points and the switch. In general, however, the overturning variations from the noise carry the pCO_2 over the transition points so that the switching behavior in the model is not as dependent on the slow pCO_2 drawdown from volcanism and weathering.

[61] In Figure 6d the scale factor for the random multiplier in (8) is increased by 50% from 1.5 to 2.25. A timescale comes out in this case that is not dependent on the slow pCO_2 drawdown at all. The new timescale is determined by the $CO_3^=$ adjustment in the deep ocean, as will be shown in the next section. This leaves the time series with high-CO_2 and low-CO_2 intervals that persist for 30 to 70,000 years with a mean value of about 50,000 years.

5.3. Origin of the 100,000-Year Cycle

[62] Figures 7 and 8 contrast two intervals in the model run from Figure 6c. In the first of these intervals (Figure 7) the model manages to produce consecutive 100,000-year cycles. In the second (Figure 8) the model produces a pair of cycles that are considerably longer. The top plots in Figures 7 and 8 show the atmospheric pCO_2. The middle plots show the deep $CO_3^=$. The bottom plots show the average TCO_2 for the whole ocean.

[63] The $CO_3^=$ time series in Figure 7 (middle) is noisy (because of the variations in f_{pd}) but the background or average $CO_3^=$ is clearly swinging above and below its long-term mean every 50,000 years or so. More importantly, the background variation is anticipating the pCO_2 transitions, as it crosses over the steady state value just before the pCO_2 transitions in the top panel take place.

[64] The situation in Figure 8 is different. The model during this time interval is clearly waiting for volcanism and weathering to bring the pCO_2 within range of the transition points at 220 and 240 ppm. Transitions in the deep $CO_3^=$ in the middle panel occur at the same time as the pCO_2 transitions in the top panel. Variations in the $CO_3^=$ background are not as large as in Figure 7 and there is no sense in which the $CO_3^=$ is anticipating the pCO_2 transitions. The average TCO_2 in Figure 8 (bottom) continues to rise or fall right up to the time that the pCO_2 hits the transition points.

[65] So, why is the situation so different between these two time periods? Basically, the model is producing a new interaction in Figure 7. The new interaction is derived from the mutual effects that the $CaCO_3$ burial and the southern ventilation are having on each other. The random fluctuations happen to be large and/or frequent enough during this interval to initiate some semblance of this mutual enhancement in the model.

[66] During the first 10,000 or 20,000 years after a transition into a cold, low-CO_2 state the deep $CO_3^=$ is well below its long-term mean. The low $CO_3^=$ suppresses the burial of $CaCO_3$ so that the ocean is gaining more alkalinity from weathering than it is losing to $CaCO_3$ burial. The net alkalinity increase keeps a slight downward pressure on the pCO_2. A positive fluctuation at this point may raise the pCO_2 but it does not set off a transition because the nascent pCO_2 increase is opposed by the increase in alkalinity. The next

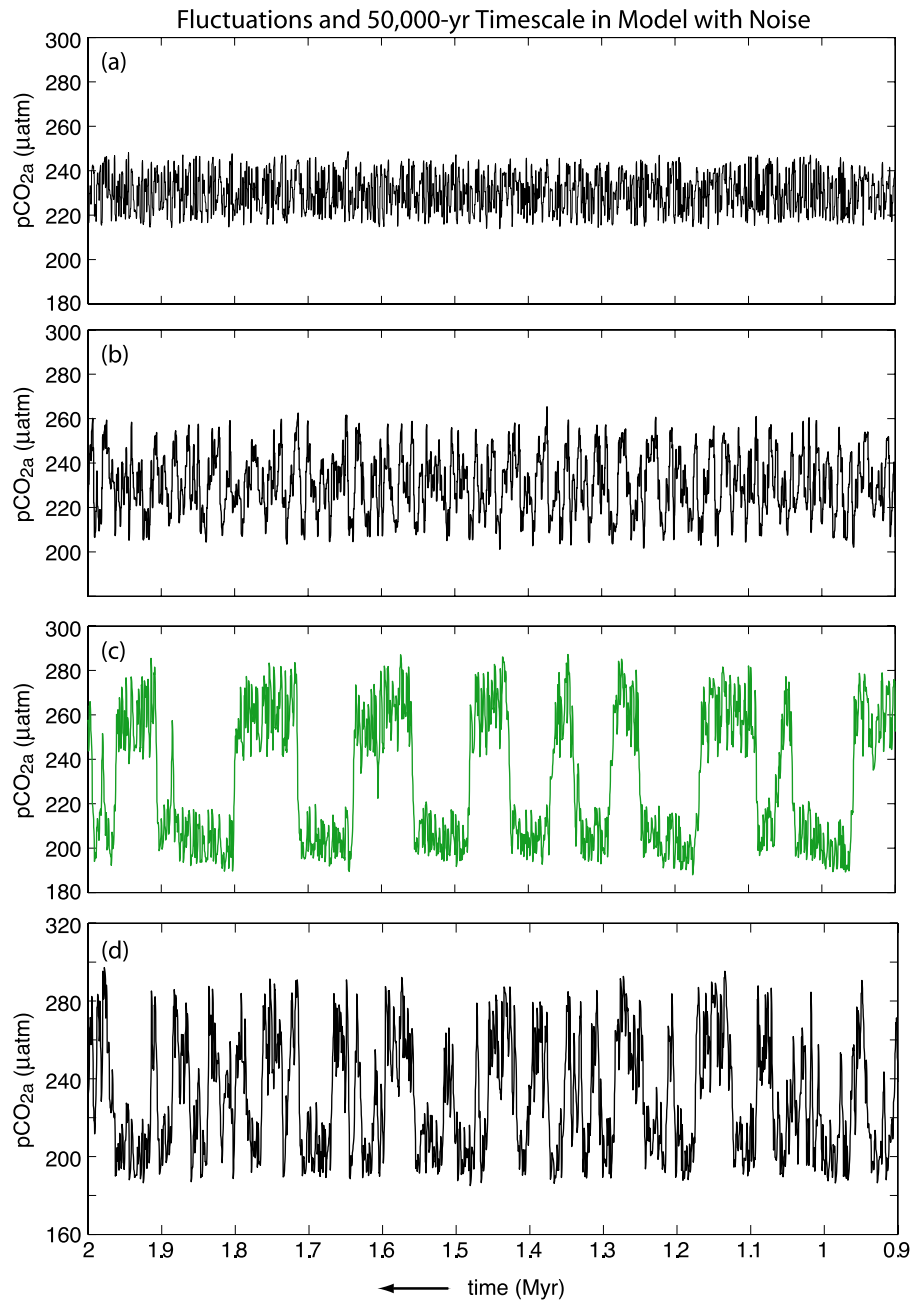**Figure 6.** Development of the 100,000-year cycle and 50,000-year timescale. Atmospheric $p\mathrm{CO_2}$ time series are shown from four versions of the model: (a) with the noise and the weathering feedback operating alone, (b) with the ventilation switch added, (c) with $\mathrm{CO_3^=}$ damping active in the deep box (in green), and (d) as in Figure 6c with the amplitude of the noise increased by 50%. See text for discussion.

negative fluctuation to come along pulls the $p\mathrm{CO_2}$ back down.

[67] The situation is different 30,000 years later. The $\mathrm{CO_3^=}$ has risen to the point where the alkalinity loss due to $\mathrm{CaCO_3}$ burial has more or less come back into balance with the alkalinity input from weathering. A positive fluctuation at this point flips the system over to a state where the alkalinity loss due to $\mathrm{CaCO_3}$ burial exceeds the input from weathering.

The loss of alkalinity from the ocean in this case reinforces the nascent $p\mathrm{CO_2}$ increase. The $p\mathrm{CO_2}$ increase then warms the atmosphere in a way that enhances the southern ventilation and the venting of respired $\mathrm{CO_2}$. This further enhances the burial of $\mathrm{CaCO_3}$, etc. In this way, a fluctuation that comes along as the weathering and $\mathrm{CaCO_3}$ burial come back into balance is converted into a big transition.
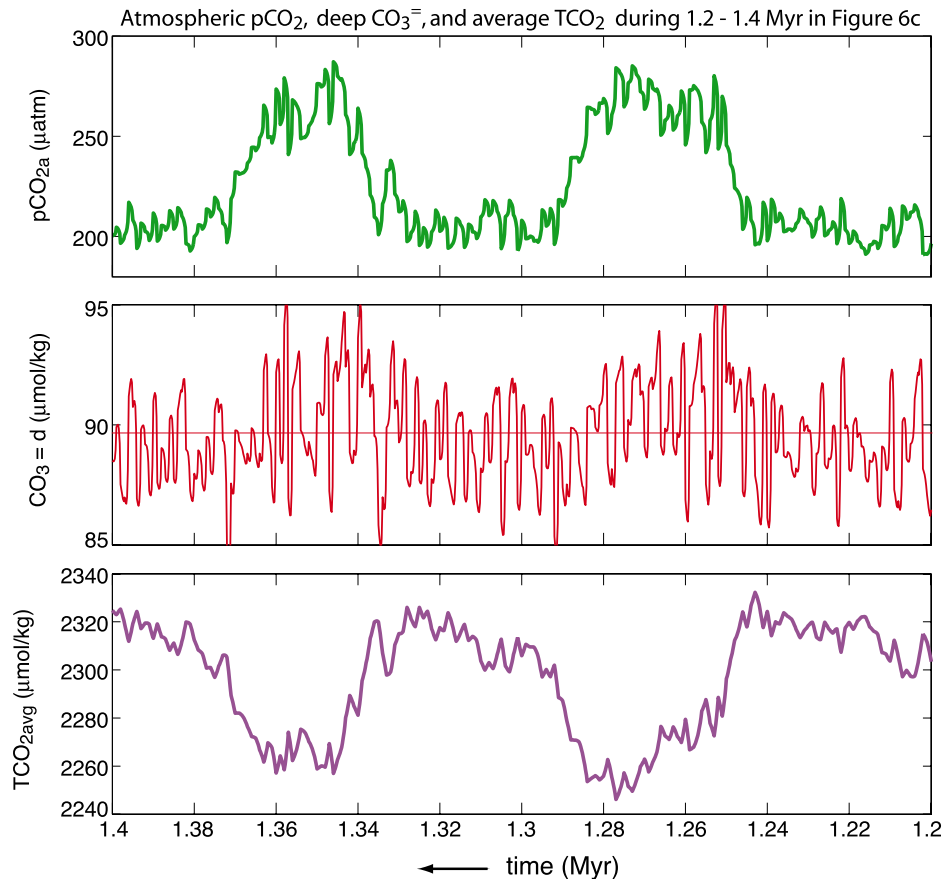
Figure 7. Detail of interval between 1.2 and 1.4 Ma in Figure 6c (green record): (top) atmospheric pCO_2, (middle) deep box $CO_3^=$, and (bottom) average oceanic TCO_2. The model during this time period produces consecutive 100,000-year cycles in which the background variations of the deep $CO_3^=$ cross over the mean $CO_3^=$ (middle plot) ahead of the major transitions in the pCO_2 (top plot). The crossover times during this interval are 50,000 years apart. They signal a change in the burial of $CaCO_3$ in relation to the weathering on land, which converts relatively minor pCO_2 fluctuations into major transitions.

[68] This sort of transition via feedback is similar to basic idea of *Toggweiler et al.* [2006], which incorporates the overturning around Antarctica, the release of respired CO_2, and shifts in the midlatitude westerly winds. The feedback here inserts $CaCO_3$ more explicitly into the loop and, as such, is able to explain why certain overturning fluctuations 50,000 years apart lead to transitions while most do not.

[69] The feedback of *Toggweiler et al.* [2006] presupposes a fairly strong greenhouse effect in which small ventilation and pCO_2 changes can be augmented by the feedback. The feedback here only gets underway when the enhanced burial of $CaCO_3$ leads to larger pCO_2. As such, the modified feedback here requires less greenhouse warming per unit of additional CO_2.

5.4. Distinction Between $CaCO_3$ Compensation and the Internal Mechanism

[70] Ventilation of the deep ocean takes respired CO_2 from the deep ocean and adds it to the atmosphere. This extraction raises the $CO_3^=$ content of the deep ocean and

makes it a more favorable environment for the burial of $CaCO_3$. The increased burial of $CaCO_3$ removes alkalinity from the ocean and raises the atmospheric pCO_2 by an additional amount.

[71] *Broecker and Peng* [1987] assumed that the $CO_3^=$ increase in the deep ocean would be erased within a few thousand years by the enhanced burial of $CaCO_3$. They imagined that most of the $CaCO_3$ delivered to the seafloor during this interval would be preserved and buried. Removing $CaCO_3$ in this way takes two units of alkalinity from the ocean for every unit of CO_2.

[72] In the internal mechanism, there is a secondary $CO_3^=$ increase during glacial-interglacial transitions that occurs in stages through the feedback. (Renewed ventilation enhances the burial of $CaCO_3$ and the pCO_2, but, in this case, the enhanced pCO_2 enhances the ventilation further, which leads to more $CaCO_3$ burial, a higher pCO_2, etc.) So, even though a large amount of $CaCO_3$ is removed during a transition, the deep ocean is left with a small secondary excess of $CO_3^=$ at the
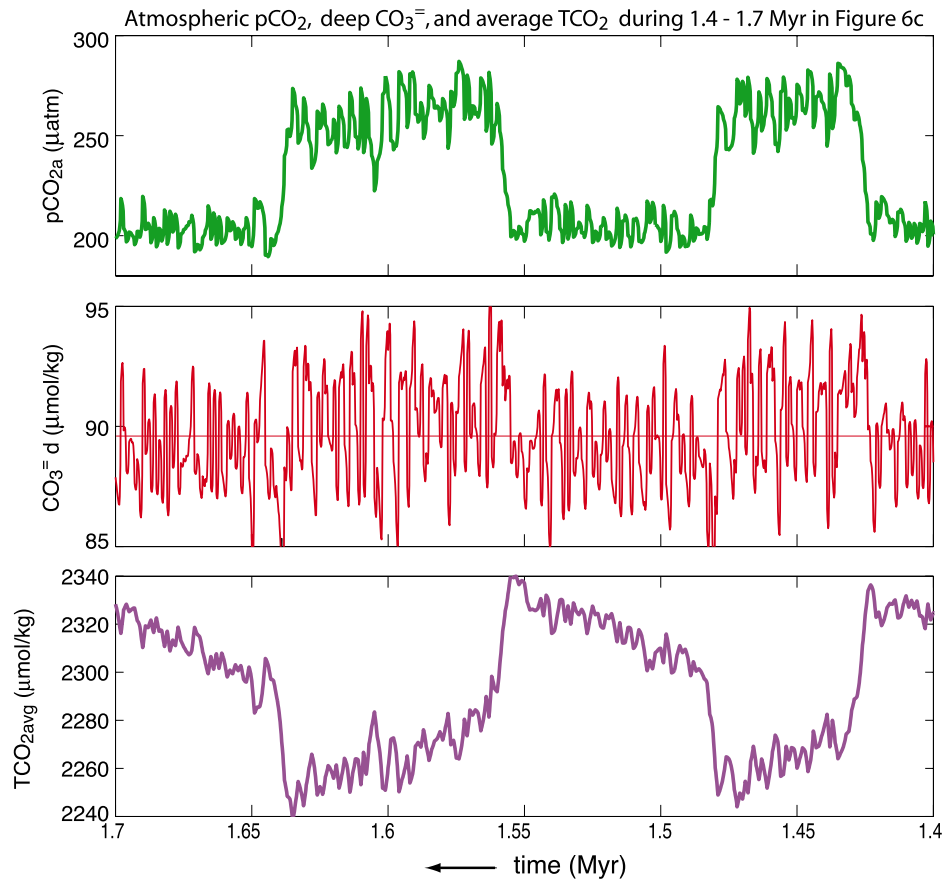
Figure 8. Detail of interval between 1.4 and 1.7 million years in Figure 6c (green record): (top) atmospheric pCO$_2$, (middle) deep box CO$_3^=$, and (bottom) average oceanic TCO$_2$. The model fails to produce the 100,000-year cycles seen in Figure 7 during this interval as the system is left waiting for volcanism and weathering to draw the pCO$_2$ within range of the transition points at 220 and 240 ppm. Encounters with the transition points determine the cycle time rather than changeovers in the deep CO$_3^=$.

end of the feedback phase, which can be seen in the elevated background at 1.255 and 1.345 Ma in Figure 7 (middle).

[73] The secondary CO$_3^=$ excess at the end of the feedback phase is erased over tens of thousands of years, rather than a few thousand years, through a process in which a little more than one unit of alkalinity is removed from the ocean for every unit of TCO$_2$. A lower ratio is obtained because every unit of alkalinity that is lost through CaCO$_3$ burial is offset, in this case, by an input of alkalinity from silicate weathering. The timescale for the secondary CO$_3^=$ excess to be drawn down reflects the throughput of CO$_2$ through the system rather than the gross delivery of CaCO$_3$ to the seafloor. Roughly 50,000 years, or 10% of the throughput time, is needed for the secondary excess to be drawn down via this process.

5.5. Parameter Sensitivity in the Model

[74] Much of the behavior of the model in this paper is dictated by a parameters and rules that have limited applicability to the real world. The timing of the model's pCO$_2$ changes, in particular, is sensitive to the spread between the transition points at 220 and 240 ppm and the amplitude of the fluctuations, as seen in Figure 6. Independent variation of these parameters has no significance outside of the model.

[75] The maximum and minimum values of the atmospheric pCO$_2$ are set to a large extent by the maximum and minimum values of f$_{pd}$ in Table 1. These limits on f$_{pd}$ limit the degree to which the southern ventilation in the model can interact with changes in CaCO$_3$ burial. This means that the mutual variability between the southern ventilation and the burial of CaCO$_3$ could easily be greater in the real world than in the model.

[76] Two parameter choices in the model deserve some mention. One is the 5000-year damping time for CO$_3^=$ set by WDAMP in (5). The nominal damping time for the deep CO$_3^=$ is noteworthy for how little impact it has. Reducing the damping time in (5) from 5,000 years to 20,000 years allows the deep CO$_3^=$ variations to become larger, and it reduces the atmospheric pCO$_2$ variations somewhat by reducing the maximum rates at which CaCO$_3$ is buried and dissolved, but it has no impact on the duration of the model's CO$_2$ cycles.
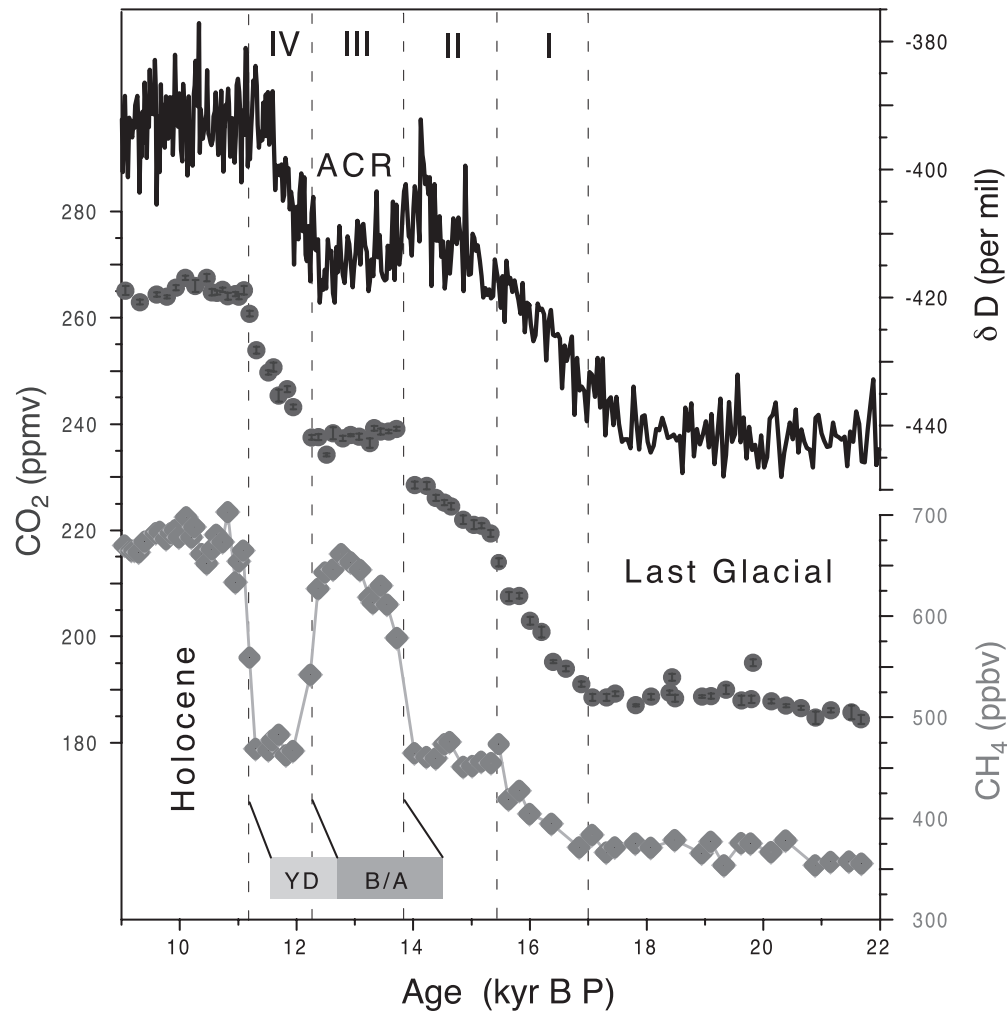
Figure 9. Detail of the CO_2 (middle curve) and Antarctic temperature increases (top curve) during the last glacial-interglacial transition. ACR is Antarctic Cold Reversal. From *Monnin et al.* [2001]. Reprinted with permission from AAAS (www.sciencemag.org).

[77] Control over the timescale lies with the parameters that control the throughput of CO_2 — the volcanic CO_2 source, VDG, and the silicate weathering parameters, BSIL and WSIL, in (2). Given the current best estimate for the volcanic CO_2 output [*Marty and Tolstikhin*, 1998], it should take about 500,000 years to turnover all the CO_2 in the ocean-atmosphere system. Ten percent of the turnover time is 50,000 years. If VDG and WSIL are increased together so that the steady state pCO_2 stays the same but the CO_2 turnover is speeded up, the $CO_3^=$ adjustment time can be shortened to, say, 35,000 years and the 100,000-year cycle can be shortened to 70,000 years.

6. Discussion

6.1. Overturning Fluctuations in the Real World

[78] Well-resolved fluctuations are observed in the overturning around Antarctica that warm and cool Antarctica while changing the atmospheric pCO_2. The temperature and CO_2 changes associated with the fluctuations are about one fourth or one third as large as those in the big transitions. Recent observations show that the most recent glacial-interglacial transition was initiated by one of these fluctuations, and the CO_2 increase that followed was augmented by a big increase in $CaCO_3$ burial.

[79] Figure 9 shows a detail of the temperature and CO_2 increases between 17,000 and 11,000 years ago during the transition out of the most recent cold period [after *Monnin et al.*, 2001]. The temperature over Antarctica seems to have increased in two steps (top curve of Figure 9), along with the atmospheric pCO_2 (middle curve). The first step in Figure 9 raised the pCO_2 by about 40 ppm. The suggestion here is that the first step was initiated by a positive fluctuation in the overturning/ventilation that warmed Antarctica and allowed respired CO_2 to vent from the deep ocean at the same time.

[80] Seven other episodes of Antarctic warming took place between 35 and 85 ka B.P. (events A1 through A7 in Figure 10 [*Blunier and Brook*, 2001]). Events A1–A4
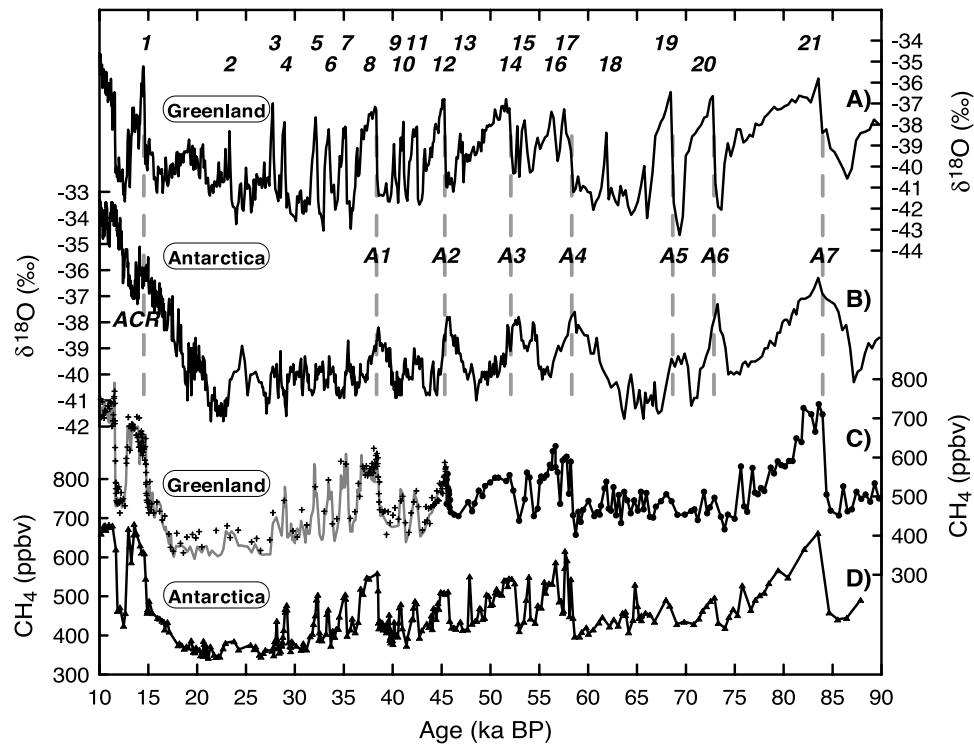
Figure 10. Comparison of temperature variations in Greenland and Antarctica over the last 85,000 years. From *Blunier and Brook* [2001]. Reprinted with permission from AAAS (www.sciencemag.org).

coincided with 20–30 ppm increases in atmospheric CO_2 [*Indermühle et al.*, 2000]. (A similarly detailed CO_2 record is not available for events A5–A7). Successive temperature and CO_2 increases were about 5,000 to 10,000 years apart and were also presumably responses to fluctuations in the overturning around Antarctica. In each of these cases warming gave way to cooling, i.e., positive fluctuations were followed by negative fluctuations.

[81] A proxy for the ocean's deep $CO_3^=$ given by *Marchitto et al.* [2005] shows that the deep $CO_3^=$ in the tropical Pacific was low during the interval between 20,000 and 70,000 years B.P. The deep $CO_3^=$ then jumped up with the start of the first CO_2 step in Figure 9 and reached a maximum about 10,000 years later, a few thousand years after the second CO_2 step. Thus, the two steps in Figure 9 occurred along with a huge increase in the burial of $CaCO_3$, while the earlier CO_2 increases associated with A1–A4 in Figure 10 did not.

[82] *Jaccard et al.* [2005] show that there were huge spikes in $CaCO_3$ preservation in the deep North Pacific that mark the loss of CO_2 from the deep ocean at the last five glacial-interglacial transitions. These are the only times that a significant amount of $CaCO_3$ is preserved at the site. This demonstrates that cold-to-warm transitions are definitely a special time with respect to the burial of $CaCO_3$.

[83] The two steps in Figure 9 are separated by an interval in which the temperature fell slightly and the pCO_2 was basically flat. The temperature dip is known as the Antarctic Cold Reversal (ACR). The ACR was presumably the response to a weakening of the overturning after the positive

fluctuation that initiated the first step. The ongoing burial of $CaCO_3$ at this time almost certainly helped maintain the pCO_2 when the overturning weakened.

[84] With this higher pCO_2, Antarctica and the Southern Ocean stayed warmer than they might otherwise have been. The warmer temperatures, reduced sea ice, and the poleward shifted westerlies in this semiwarm state in turn, limited the weakening of the overturning. When the overturning resumed, Antarctica began warming from a warmer intermediate state. The feedback was presumably in control at this point and carried Antarctica to its modern interglacial state. It is noteworthy in this regard that the interval of enhanced $CaCO_3$ burial, which can be inferred from the elevated $CO_3^=$ given by *Marchitto et al.* [2005], persists through the two steps and beyond.

[85] The Antarctic Cold Reversal in Figure 9 coincides with the Bolling-Allerod (B/A), the first deglacial warm interval in the north. The two warming steps in Figure 9 and the warming episodes in Figure 10 all took place while Greenland was cooling. Four of the warming events occurred along with Heinrich Events in the North Atlantic. This out-of-phase warming between the hemispheres seems to be characteristic of all the overturning fluctuations during this time.

[86] The out-of-phase warming is often described as a "seesaw" in which the ocean's overturning brings warm water alternately to the two poles [*Broecker*, 1998]. The seesaw is usually seen as a forced phenomenon in which inputs of fresh water in the North Atlantic shut down the

formation of deep water in the north. The overturning in the south then switches on in response to the forced shutdown in the north [*Ganopolski and Rahmstorf*, 2001].

[87] On the other hand, the seesaw could simply be a particular manifestation of the unstable overturning that has prevailed over the last million years. If so, changes in the seesaw could start in either hemisphere and could be triggered by noise in the system rather than specific forcing events.

6.2. Correlation, Causation, and the CO_2 Lead Over Ice Volume

[88] The temporal correlation between atmospheric CO_2 and Antarctic temperatures in Figure 1 is often taken as an indication that there is a big greenhouse role for CO_2 in the 100,000-year cycle [*Genthon et al.*, 1987; *Lorius et al.*, 1990; *Hansen et al.*, 2007]. The main problem with this idea is that the $8°-10°C$ temperature variations in Figure 1 are very large in relation to the warming and cooling expected from 100-ppm CO_2 changes [*Broccoli and Manabe*, 1987]. The fact that Antarctic temperatures seem to increase ahead of CO_2 at the big transitions [*Fischer et al.*, 1999; *Caillon et al.*, 2003] suggests that the CO_2-temperature relationship is not causal.

[89] The idea presented here is that the overturning, the winds, and sea ice do most of the work to change the temperatures over Antarctica. The greenhouse forcing from CO_2 is part of the feedback but would not seem to be warming Antarctica very much by itself. The two records are correlated simply because Antarctic temperatures and atmospheric CO_2 are responding in a similar way to the internal mechanism. Antarctic temperatures increase slightly ahead of CO_2 because the venting of CO_2 up to the atmosphere is delayed by gas exchange and the ongoing burial of $CaCO_3$ [*Toggweiler et al.*, 2006].

[90] *Lea et al.* [2000], *Visser et al.* [2003], and *Lea* [2004] have shown that temporal variations in sea surface temperatures (SSTs) in the equatorial Pacific are also highly correlated with CO_2. Again, the relationship is often seen as causal. The SST variations in the equatorial Pacific have a maximum amplitude of about $4°C$ [*Lea*, 2004], which is $25-30\%$ larger than the warming and cooling expected from CO_2 and the other greenhouse gases.

[91] Most of the temperature variation in the equatorial records is associated with the abrupt warmings at the major transitions. These warm spikes tend to be brief, like those in Antarctica. The suggestion here is that some of the warming in these deglacial temperature spikes is due to atmospheric and oceanic circulation changes that have reached the tropical Pacific from Antarctica and the Southern Ocean. Thus, some of the temperature variation in the equatorial Pacific may very well be correlated with CO_2 but is not actually a response to CO_2.

[92] It is often noted in this regard that equatorial SSTs, CO_2, and Antarctic temperatures lead the $\delta^{18}O$ decreases at glacial terminations by a few thousand years. The lead is usually seen as being highly significant in the causal sense: CO_2 goes up and slowly warms the oceans; the northern ice sheets begin melting in earnest as the ocean warms.

[93] In the scenario put forward in the next section, section 6.3, the ice sheets melt back primarily in response

to regular variations in summer insolation [*Roe*, 2006]. CO_2, on the other hand, goes up initially in response to a random fluctuation in the overturning around Antarctica. This means that the CO_2 lead over ice volume could vary considerably from one termination to the next. A CO_2 lead that varies in this way is probably not highly significant.

[94] CO_2 can presumably introduce some 100,000-year variability into the northern ice sheets without actually melting back the ice sheets at terminations. High CO_2 levels may retard ice sheet development when cool northern summers would otherwise be conducive to ice sheet growth, during isotope stage 5d, for example. Similarly, low CO_2 may help the ice sheets become extra large when the eccentricity is low and the summer insolation is not so extreme, as in isotope stages 2 and 3. The extra ice then melts away when the summer insolation becomes strong again.

6.3. Distinct Climate Variations in the Northern and Southern Hemispheres

[95] The internal mechanism and its 100,000-year time-scale are local to Antarctica. This implies that the climate variations around Antarctica are fundamentally different from those in the Northern Hemisphere. It also leads one to suspect that the ice ages in the north have less 100,000-year variability.

[96] The currently accepted explanation for the ice ages, the astronomical theory of *Milankovitch* [1930], is focused on the Northern Hemisphere. It attributes the waxing and waning of the northern ice sheets to periodic variations in the Earth's orbit and spin axis that alter the northern summer insolation. The forcing in this case comes primarily from variations in the precession of the Earth's axis every 23,000 years and variations in the obliquity (tilt) of the axis every 41,000 years.

[97] The simplest form of the theory says that the ice sheets should respond in a linear way to the northern summer insolation [*Hays et al.*, 1976], in which case the largest ice sheet variations would appear after the largest insolation extremes every 23,000 years or every 41,000 years. This is not what Hays et al. found. Using the $\delta^{18}O$ variations in marine carbonate shells as a proxy for ice volume, Hays et al. found that only 40% of the total variance in ice volume occurs in frequency bands with periods of 23,000 and 41,000 years; 60% of the total variance is concentrated in a frequency band with a period near 100,000 years.

[98] *Hays et al.* [1976] suggested that the 100,000-year cycle is a nonlinear response to the eccentricity of the Earth's orbit, which varies over 100,000 years but has a small direct effect on insolation. In support of this argument, Hays *et al.* showed that glacial periods (with heavy $\delta^{18}O$) have tended to fall during times of low eccentricity. They felt that the in-phase relationship between maximum ice and low eccentricity indicated that the orbital forcing is the "pacemaker" of the ice ages in all three frequency bands.

[99] A more substantial forcing agent was identified a decade later with the discovery of the CO_2 variations in Figure 1 [*Barnola et al.*, 1987]. Atmospheric CO_2 seems to be increasing while the eccentricity is increasing [*Shackleton*, 2000] and it appears to be melting back the ice sheets in a way that could fit within the Milankovitch frame-

work. Bringing CO_2 into the framework, of course, begs the question of why CO_2 should be responding to the eccentricity in the first place. The forcing due to 100-ppm variations in atmospheric CO_2 is also not very strong in relation to the forcing from precession and tilt [*Roe*, 2006]. Why should the ice sheets be responding so strongly to two relatively weak forcing agents over this time period?

[100] *Shackleton*'s [1987, 2000] basic insight was to see that much of the 100,000-year variability (and much of the sawtooth shape) in the marine $\delta^{18}O$ record comes from temporal variations in ocean temperatures that are distinct from the temporal variations in northern ice volume. When the temperature effect is taken away, more of the total variance in northern ice volume is in the precession and obliquity bands. This makes the actual ice sheet response in the north more like the forcing.

[101] The suggestion here is that most of the 100,000-year temperature variability in the ocean is a greenhouse response to CO_2 cycles from the south, as given by *Shackleton* [2000]. There is also some additional 100,000-year variability in the Southern Hemisphere and equatorial Pacific that is a remote response to the non-greenhouse parts of the internal mechanism. The big warmings in Antarctica, on the other hand, are primarily a local response to the overturning changes, wind shifts, and sea ice changes that are the core parts of the internal mechanism. This big local component allows Antarctica to warm ahead of CO_2 during the big transitions. It also allows the temperature variability in Antarctica to stand out above the local responses to precession and tilt in the south [*Petit et al.*, 1999].

[102] Taken together, the Northern and Southern Hemispheres would seem to have dominant influences and dominant periods of variability that are basically independent: precession and tilt make the ice sheets grow and shrink in the north; the internal mechanism warms and cools the south. The greenhouse effect from the internal mechanism in the south transmits some of the 100,000-year southern variability to the northern ocean and the northern ice sheets but the northern variability should be small in relation to the 100,000-year variability in Antarctica.

[103] The greater land area in the Northern Hemisphere leads to a monsoonal response to the precessional forcing and to regular changes in atmospheric methane [*Ruddiman and Raymo*, 2003]. It is telling in this regard that there are small maxima in Antarctic temperatures that line up with the maxima in atmospheric methane [*Petit et al.*, 1999]. This observation demonstrates that there is a precessional influence in the south with a Northern Hemisphere phase.

[104] This last bit of information helps explain, perhaps, why the 100,000-year cycle in the south comes to be in phase with eccentricity. Two cycles can easily become phase locked if they happen to have the same period. Information about the phase of one of the cycles simply has to be picked up by the other [*Tziperman et al.*, 2006]. In this case, the internal cycle coincidentally has the same period as the eccentricity. Information about the phase of the eccentricity cycle passes across the equator via atmospheric methane. When the northern

precession cycles are stronger during times of maximum eccentricity, the greenhouse effect from atmospheric methane may subtly warm the south in a way that helps to initiate the southern feedback at times when the eccentricity of the Earth's orbit is increasing.

7. Conclusions

[105] The abrupt warmings and the big CO_2 increases recorded in Antarctic ice cores occur through an internal mechanism with an internal 100,0000-year timescale. The root of the internal mechanism is the unstable overturning in the ocean around Antarctica.

[106] The most recent transition began with a seesaw-like fluctuation in the overturning around Antarctica [*Monnin et al.*, 2001], which released respired CO_2 from the deep ocean up to the atmosphere [*Marchitto et al.*, 2007]. The CO_2 release at this particular time flipped a $CO_3^=$ deficit in the deep ocean into a $CO_3^=$ excess [*Marchitto et al.*, 2005], which led to an enhancement in the ocean's $CaCO_3$ burial that augmented the atmospheric CO_2 increase. Warming from the elevated CO_2 then led to more overturning, which led to still more CO_2 in the atmosphere and more $CaCO_3$ burial, etc. In this way, the internal feedback and the burial of $CaCO_3$ converted a relatively minor overturning fluctuation into a major transition.

[107] The feedback idea put forward here is similar to one given by *Toggweiler et al.* [2006]. The difference here is that the enhanced burial of $CaCO_3$ sets off the feedback rather than the initial release of respired CO_2. Transitions that take place through the feedback leave the deep ocean with an excess of $CO_3^=$ that is erased over $40-50,000$ years. Changeovers in the burial of $CaCO_3$ at the ends of these intervals set up the next transition. The time needed to erase the $CO_3^=$ excess is roughly the turnover time for the $CO_3^=$ ions in the ocean with respect to the weathering of silicate rocks and the associated burial of $CaCO_3$ on the seafloor, which is 10% of the overall turnover time for CO_2.

[108] The internal mechanism warms and cools the whole planet via the CO_2 greenhouse effect but local overturning changes, sea ice changes and wind shifts around Antarctica warm and cool Antarctica to a greater degree. Because the temperature increases in Antarctica seem to take place ahead of the CO_2 increases it would appear that the local effects have more impact than the greenhouse effect. This is important because the way that the temperature changes are apportioned in Antarctica (local versus greenhouse) limits how large the 100,000-year temperature changes over the rest of the Earth can be. These considerations suggest that Northern Hemisphere temperature variations are much smaller over 100,000 years than those in and around Antarctica and that the northern ice sheets respond more strongly to precession and tilt than to CO_2 [*Roe*, 2006].

[109] The ideas in this paper have their origin in a simple model that produces more-or-less symmetric transitions between the "warm" and "cold" states of the CO_2 system. As such, the model does not explain the sawtooth shape of the 100,000-year cycle. It would seem fairly obvious in this context that the sawtooth exists because the "warm" transi-

tions of the internal mechanism produce bigger changes in $CaCO_3$ than the "cold" transitions [*Jaccard et al.*, 2005]. An explanation for why this is so is left to future work.

References

Barnola, J. M., D. Raynaud, Y. S. Korotkevich, and C. Lorius (1987), Vostok ice core provides 160,000-year record of atmospheric CO_2, *Nature*, *329*, 408–414, doi:10.1038/329408a0.

Berner, R. A. (1991), A model for atmospheric CO_2 over Phanerozoic time, *Am. J. Sci.*, *291*, 339–376.

Berner, R. A. (1998), The carbon cycle and CO_2 over Phanerozoic time: The role of land plants, *Philos. Trans. R. Soc. London, Ser. B*, *353*, 75–82, doi:10.1098/rstb.1998.0192.

Blunier, T., and E. J. Brook (2001), Timing of millennial-scale climate change in Antarctica and Greenland during the last glacial period, *Science*, *291*, 109–112, doi:10.1126/science.291.5501.109.

Broccoli, A. J., and S. Manabe (1987), The influence of continental ice, atmospheric CO_2, and land albedo on the climate of the last glacial maximum, *Clim. Dyn.*, *1*, 87–99, doi:10.1007/BF01054478.

Broecker, W. S. (1982), Glacial to interglacial changes in ocean chemistry, *Prog. Oceanogr.*, *11*, 151–197, doi:10.1016/0079-6611(82)90007-6.

Broecker, W. S. (1998), Paleocean circulation during the last deglaciation: A bi-polar seesaw?, *Paleoceanography*, *13*, 119–121, doi:10.1029/97PA03707.

Broecker, W. S., and T.-H. Peng (1987), The role of $CaCO_3$ compensation in the glacial to interglacial atmospheric CO_2 change, *Global Biogeochem. Cycles*, *1*, 15–29.

Broecker, W. S., and J. van Donk (1970), Insolation changes, ice volumes, and the ^{18}O record in deep-sea cores, *Rev. Geophys. Space Phys.*, *8*, 169–198, doi:10.1029/RG008i001p00169.

Caillon, N., J. P. Severinghaus, J. Jouzel, J.-M. Barnola, J. Kang, and V. Y. Lipenkov (2003), Timing of atmospheric CO_2 and Antarctic temperature changes across Termination III, *Science*, *299*, 1728–1731, doi:10.1126/science.1078758.

de Boer, A. M., D. M. Sigman, J. R. Toggweiler, and J. L. Russell (2007), Effect of global ocean temperature change on deep ocean ventilation, *Paleoceanography*, *22*, PA2210, doi:10.1029/2005PA001242.

Fischer, H., M. Whalen, J. Smith, D. Mastroianni, and B. Deck (1999), Ice core records of atmospheric CO_2 around the last three glacial terminations, *Science*, *283*, 1712–1714, doi:10.1126/science.283.5408.1712.

Ganopolski, A., and S. Rahmstorf (2001), Rapid changes of glacial climate simulated in a coupled climate model, *Nature*, *409*, 153–158, doi:10.1038/35051500.

Genthon, G., J. M. Barnola, D. Raynaud, C. Lorius, J. Jouzel, N. I Barkov, Y. S. Korotkevich, and V. M. Kotlyakov (1987), Vostok ice core: Climate response to CO_2 and orbital forcing changes over the last climate cycle, *Nature*, *329*, 414–418, doi:10.1038/329414a0.

Hansen, J., M. Sato, P. Kharecha, G. Russell, D. W. Lea, and M. Siddall (2007), Climate change and trace gases, *Philos. Trans. R. Soc., Ser A*, 1925–1954.

Hays, J. D., J. Imbrie, and N. J. Shackleton (1976), Variations in the Earth's orbit: Pacemaker of the ice ages, *Science*, *194*, 1121–1132, doi:10.1126/science.194.4270.1121.

Hodell, D. A., K. A. Venz, C. D. Charles, and U. S. Ninnemann (2003), Pleistocene vertical carbon isotope and carbonate gradients in the South Atlantic sector of the Southern Ocean, *Geochem. Geophys. Geosyst.*, *4*(1), 1004, doi:10.1029/2002GC000367.

Imbrie, J., et al. (1984), The orbital theory of Pleistocene climate: Support from a revised chronology of the marine $\delta^{18}O$ record, in *Milankovitch and Climate*, part 1, edited by A. Berger et al., pp. 269–305, Springer, Dordrecht, Netherlands.

Indermühle, A., E. Monnin, B. Stauffer, and T. F. Stocker (2000), Atmospheric CO_2 concentrations from 60 to 20 kyr BP from the Taylor Dome ice core, Antarctica, *Geophys. Res. Lett.*, *27*(5), 735–738, doi:10.1029/1999GL010960.

Jaccard, S. L., G. H. Haug, D. M. Sigman, T. F. Pedersen, H. R. Thierstein, and U. Röhl (2005), Glacial/interglacial changes in subarctic North Pacific stratification, *Science*, *308*, 1003–1006, doi:10.1126/science.1108696.

Lea, D. W. (2004), The 100,000-yr cycle in tropical SST, greenhouse forcing, and climate sensitivity, *J. Clim.*, *17*(11), 2170–2179, doi:10.1175/1520-0442(2004)017<2170:TYCITS>2.0.CO;2.

Lea, D. W., D. K. Pak, and H. J. Spero (2000), Climate impact of late Quaternary equatorial Pacific sea surface temperature variations, *Science*, *289*, 1719–1724, doi:10.1126/science.289.5485.1719.

Lorius, C., J. Jouzel, D. Raynaud, J. Hansen, and H. Le Treut (1990), The ice core record: Climate sensitivity and future greenhouse warming, *Nature*, *347*, 139–145, doi:10.1038/347139a0.

Lowenstein, T. K., and R. V. Demicco (2006), Elevated Eocene atmospheric CO_2 and its subsequent decline, *Science*, *313*, 1928, doi:10.1126/science.1129555.

Marchitto, T. M., J. Lynch-Stieglitz, and S. R. Hemming (2005), Deep Pacific $CaCO_3$ compensation and glacial-interglacial CO_2, *Earth Planet. Sci. Lett.*, *231*, 317–336, doi:10.1016/j.epsl.2004.12.024.

Marchitto, T. M., S. J. Lehman, J. D. Ortiz, J. Fluckiger, and A. van Geen (2007), Marine radiocarbon evidence for the mechanism of deglacial atmospheric CO_2 rise, *Science*, *316*, 1456–1459, doi:10.1126/science.1138679.

Marty, B., and I. N. Tolstikhin (1998), CO_2 fluxes from mid-ocean ridges, arcs, and plumes, *Chem. Geol.*, *145*, 233–248, doi:10.1016/S0009-2541(97)00145-9.

Milankovitch, M. (1930), *Mathematische Klimalehre und Astronomische Theorie der Klimasch-Wankungen*, 176 pp., Gebrüder Borntraeger, Berlin.

Monnin, E., et al. (2001), Atmospheric CO_2 concentrations over the last glacial termination, *Science*, *291*, 112–114, doi:10.1126/science.291.5501.112.

Moulton, K. L., and R. A. Berner (1998), Quantification of the effect of plants on weathering: Studies in Iceland, *Geology*, *26*(10), 895–898, doi:10.1130/0091-7613(1998)026<0895:QOTEOP>2.3.CO;2.

Petit, J. R., et al. (1999), Climate and atmospheric history of the past 420,000 years from the Vostok ice core, Antarctica, *Nature*, *399*, 429–436, doi:10.1038/20859.

Raymo, M. E., and W. F. Ruddiman (1992), Tectonic forcing of late Cenozoic climate, *Nature*, *359*, 117–122, doi:10.1038/359117a0.

Roe, G. (2006), In defense of Milankovitch, *Geophys. Res. Lett.*, *33*, L24703, doi:10.1029/2006GL027817.

Ruddiman, W. F., and M. E. Raymo (2003), A methane-based time scale for Vostok ice, *Quat. Sci. Rev.*, *22*, 141–155, doi:10.1016/S0277-3791(02)00082-3.

Shackleton, N. J. (1967), Oxygen isotope analyses and Pleistocene temperatures re-assessed, *Nature*, *215*, 15–17, doi:10.1038/215015a0.

Shackleton, N. J. (1987), Oxygen isotopes, ice volume, and sea level, *Quat. Sci. Rev.*, *6*, 183–190, doi:10.1016/0277-3791(87)90003-5.

Shackleton, N. J. (2000), The 100,000-year ice age cycle identified and found to lag temperature, carbon dioxide, and orbital eccentricity, *Science*, *289*, 1897–1902, doi:10.1126/science.289.5486.1897.

Siegenthaler, U., et al. (2005), Stable carbon cycle-climate relationship during the late Pleistocene, *Science*, *310*, 1313–1317, doi:10.1126/science.1120130.

Toggweiler, J. R. (1999), Variation of atmospheric CO_2 by ventilation of the ocean's deepest water, *Paleoceanography*, *14*, 571–588, doi:10.1029/1999PA900033.

Toggweiler, J. R., R. Murnane, S. Carson, A. Gnanadesikan, and J. L. Sarmiento (2003), Representation of the carbon cycle in box models and GCMs, 2, Organic pump, *Global Biogeochem. Cycles*, *17*(1), 1027, doi:10.1029/2001GB001841.

Toggweiler, J. R., J. L. Russell, and S. R. Carson (2006), Midlatitude westerlies, atmospheric CO_2, and climate change during the ice ages, *Paleoceanography*, *21*, PA2005, doi:10.1029/2005PA001154.

Tziperman, E., M. E. Raymo, P. Huybers, and C. Wunsch (2006), Consequences of pacing the Pleistocene 100 kyr ice ages by nonlinear phase locking to Milankovitch forcing, *Pa-*

leoceanography*, *21*, PA4206, doi:10.1029/2005PA001241.

Visser, K., R. Thunell, and L. Stott (2003), Magnitude and timing of temperature change in the Indo-Pacific warm pool during deglaciation, *Nature*, *421*, 152–155, doi:10.1038/nature01297.

Walker, J. C. G., and J. F. Kasting (1992), Effect of fuel and forest conservation on future levels of atmospheric carbon dioxide, *Palaeogeogr.*

Palaeoclimatol. Palaeoecol., *97*, 151–189, doi:10.1016/0031-0182(92)90207-L.

Walker, J. C. G., P. B. Hays, and J. F. Kasting (1981), A negative feedback mechanism for the long-term stabilization of Earth's surface temperature, *J. Geophys. Res.*, *86*, 9776–9782, doi:10.1029/JC086iC10p09776.

Zachos, J., M. Pagani, L. Sloan, E. Thomas, and K. Billups (2001), Trends, rhythms, and aberrations

in global climate 65 Ma to present, *Science*, *292*, 686–693, doi:10.1126/science.1059412.

—————————————

J. R. Toggweiler, Geophysical Fluid Dynamics Laboratory, NOAA, P.O. Box 308, Princeton, NJ 08542, USA. (robbie.toggweiler@ noaa.gov)